Climate Dynamics (1993) 9:63–69

Climate Dynamics

Coupling an ocean wave model to an atmospheric general circulation model

Susanne L Weber[1], Hans von Storch[2], Pedro Viterbo[3], Liana Zambresky[4]

[1] Royal Netherlands Meteorological Institute, NL-3730 AE de Bilt, The Netherlands
[2] Max-Planck-Institute for Meteorology, Hamburg, Germany
[3] European Centre for Medium-Range Weather Forecasts Reading, Great Britain
[4] GKSS Research Centre, Geesthacht, Germany

Received: 30 September 1992/Accepted: 22 February 1993

Abstract. A coupled model, consisting of an ocean wave model and an atmospheric general circulation model (AGCM), is integrated under permanent July conditions. The wave model is forced by the AGCM wind stress, whereas the wind waves modify the AGCM surface fluxes of momentum, sensible and latent heat. We investigate the following aspects of the coupled model: how realistic are the wave fields, how strong is the coupling, and how sensitive is the atmospheric circulation to the spatially and temporally varying wave field. The wave climatology of the coupled model compares favorably with observational data. The interaction between the two models is largest (although weak) in the storm track in the Southern Hemisphere. Young windsea, which is associated with enhanced surface fluxes is generated mostly in the equatorward "frontal" area of an individual cyclone. However, the enhancement of the surface fluxes is too small to significantly modify the climatological mean atmospheric circulation.

1 Introduction

Wind waves are an obvious feature of the interface between the atmosphere and the ocean. Even with a light breeze small ripples are present on the ocean surface. Storms over the open ocean easily generate waves with wave heights in excess of 10 m. The momentum and heat fluxes through the interface are modified by the presence of waves on the interface. Ocean waves are therefore though to be of interest for climate studies, both for modeling of the atmosphere and the ocean separately and for modeling of the coupled ocean-atmosphere system (Hasselmann 1991).

This paper was presented at the Second International Conference on Modelling of Global Climate Variability, held in Hamburg 7–11 September 1992 under the auspices of the Max Planck Institute for Meteorology. Guest Editor for these papers is L. Dümenil

Correspondence to: SL Weber

In the present study detailed models of the atmospheric circulation and of the ocean wave field are coupled together. With this coupled model we investigate whether a realistic wave field is induced by the atmospheric general circulation model (AGCM), how strong the interaction between the two models is and whether the atmospheric circulation responds to the variations in the surface fluxes induced by the wave field. The atmospheric GCM and the wave model are briefly described in Section 2, with emphasis on the coupling through the sea surface roughness. The performance of the coupled model is discussed in Section 3. The simulated wave fields are compared with semi-operational wave data from the European Centre for Medium-Range Weather Forecasts (ECMWF) and the atmospheric fields are compared with fields obtained in an uncoupled control run. We summarize the results in Section 4.

2 The coupled model

The coupled model consists of the WAM wave model (WAMDIG 1989) and the ECHAM atmospheric GCM (Roeckner et al. 1992). It is integrated under permanent July conditions, so that the incoming solar radiation and the sea surface temperature do not vary. A fixed-month mode was chosen to produce time series which are long and statistically stationary, so that a meaningful statistical analysis can be performed. An integration over a longer time and in the annual-cycle mode would be preferable. Because of limited computer time this was not possible: a simulation of 30 days with the coupled WAM-ECHAM model requires 2.5 h CPU time on a Cray 2, compared to only 0.5 h for ECHAM alone.

2.1 The ocean wave model

The wave model (WAMDIG 1989) computes the local change of the wave spectrum on a regular $3° \times 3°$ grid, extending from 63°S to 81°N. It is forced by the stress

exerted by the wind on the ocean surface. The wave model describes the generation of waves by the wind, the dissipation by whitecapping, the transfer of energy within the wave spectrum by resonant four-wave interactions and the advection of energy by wave propagation. As waves grow the total energy of the wave field increases while the energy-containing range of the spectrum shifts to lower frequencies, until the wave field and the wind are in equilibrium.

A characteristic parameter of the wave field, which is commonly used, is the *significant wave height* H_s. This quantity is defined as $H_s=4\sqrt{E}$, where E is the wave variance.

Global maps of the wave height directly derived from observations do not exist. We verify our results with forecasts prepared on a semi-operational basis at the ECMWF. These forecasts were obtained by forcing the WAM model with analyzed winds from the operational ECMWF weather forecast model. The forecast wave heights have been verified extensively against various data (buoys, ship records, global satellite data), by Zambresky (1989), Bauer et al. (1992) and Romeiser (1993). These verifications show that in regions in which the wind fields are well documented, the wave height is predicted with a high degree of accuracy. In regions of poorly defined winds the wave model performs less well. Romeiser (1993), for example, shows that in the Southern Hemisphere the ECMWF wave height underestimates the real wave height by up to 20% in July. This is primarily because of too weak wind forcing.

2.2 The atmospheric general circulation model

The atmospheric GCM is the Hamburg version of the ECMWF spectral model in T21 resolution, named ECHAM (second version). A T21 spectral resolution corresponds to a horizontal resolution of about 1000 km. The model has been designed for climate studies (Roeckner et al. 1992).

In the standard ECHAM, with no wave model coupled to it, the roughness length z_0 is given over open sea by the Charnock formula (Charnock 1955):

$$z_0 = \alpha \frac{\tau}{g\rho} \tag{1}$$

with $\alpha=0.018$. Here τ is the magnitude of the turbulent stress, g is the gravitational constant and ρ is the density of air. The Charnock formula (1) is modified by a minimum condition: in the case of laminar flow (low wind speeds) z_0 is set to 0.15 mm.

The drag coefficient at height z for the neutrally stratified atmospheric boundary layer is given by:

$$c_D(z)=\{0.4/\ln(z/z_0)\}^2 \tag{2}$$

Because $\tau=\rho c_D U^2$, (1) and (2) implicitly define z_0, c_D and τ as functions of the wind speed U at height z. The drag coefficient increases with increasing wind speed. For the neutral atmosphere (2) also gives the exchange coefficient for the sensible and latent heat fluxes. In non-neutral cases the exchange coefficients for momentum and heat are modified by a factor which depends on the atmospheric stability.

2.3 The coupling of the two models

A theoretical model of wave growth due to shear flow instability of the wind has been given by Miles (1957). He assumed that the air flow and wave motion can be considered as uncoupled. Extending Miles' theory, Janssen (1989) took into account the interaction between the turbulent atmospheric boundary layer and the waves generated by it. His model of coupled wind-wave growth agrees qualitatively with observed field data (Maat et al. 1991).

The integral over all spectral components of the atmospheric momentum flux into the wave field defines the wave-induced stress (Janssen 1989). The total surface stress, thus, consists of a turbulent part and a wave-induced part. In this respect air flow over water differs from air flow over a rigid surface where there is only the turbulent stress. The wave-induced stress is large in the initial stages of wave growth, when *young* windsea prevails in the wave field. This occurs immediately after an increase in the wind speed or a change in the wind direction.

The coupling scheme used in the present experiment is based on an efficient approximation to the full coupled theory (Janssen 1991). If τ denotes the total (turbulent *and* wave-induced) stress and τ_w the wave-induced stress, then the roughness length z_0 is:

$$z_0=\beta\frac{\tau}{g\rho(1-\tau_w/\tau)^m} \tag{3}$$

In our model the parameters are $m=0.8$ and the proportionality constant $\beta=0.016$ has been chosen such that (3) reduces to the standard Charnock relation (1) for stress ratios $\tau_w/\tau=0.1$–0.2, which is the mean value in the storm track. Molecular viscosity is not considered in the theory of coupled wave growth and the minimum value for z_0 still applies. Comparing (3) to (1) it is clear that the roughness length in the coupled model depends on both the instantaneous local wind and on the wave spectrum, which is a function of the earlier wind field. The factor τ_w/τ, which depends on the wave age, denotes the strength of the coupling between wind and waves. For extreme *young* wind-sea the roughness can be enhanced by as much as a factor ten.

The discretization of the coupling scheme is as follows. At the end of every time step (40 min) of the atmospheric model ECHAM communicates the total stress to the wave model and WAM then performs the same time step (in two steps of 20 min). The resulting wave-induced stress is passed on to ECHAM. In the next time step z_0, c_D and τ are solved iteratively from U and τ_w, using (2) and (3). After taking the atmospheric stratification into account in c_D, the total surface stress is again computed from the lowest-level wind.

Wave growth affects the momentum flux at the surface. It is not clear from the theory of coupled wind-

wave growth whether the heat fluxes are also modified. Observations seem to indicate that ocean waves enhance the heat fluxes also, although the evidence is not as clear as in the case of the momentum fluxes (DeCosmo 1991). In the present experiment we compute the transfer coefficients for the sensible and latent heat fluxes from the modified roughness length (3).

3 Results

The coupled WAM-ECHAM model was integrated over 390 days. The wave fields reached a quasi-stationary state in less than 30 days. The first 30 days were therefore disregarded in the following analysis. The time-mean over the last 360 days is denoted by an overbar.

First we make a case study of a randomly chosen set of six consecutive 12-hour periods from the model (Sect. 3.1). Then, time-mean fields of the significant wave height, the wave-induced stress and the sea surface roughness (Sect. 3.2) as well as the atmospheric response to the modified sea surface conditions are discussed (Sect. 3.3).

3.1 A case study

Maps of the 12-hourly mean sea level pressure are shown in Fig. 1 together with 12-hourly mean values of the stress ratio τ_w/τ for six consecutive 12-hour periods (days 141–143). The stress ratio denotes the strength of the coupling between the waves and the atmospheric flow. In the diagrams "fronts" have been placed subjectively, even though small-scale features like fronts are not resolved by our coarse resolution GCM. The "fronts" are connected with the position of strongest horizontal temperature gradients at the 850 hPa level.

The stress ratio field is spatially and temporally highly variable. The pattern is clearly connected with the lows in the atmospheric circulation. The distribution under an individual cyclone is inhomogeneous: relatively high stress ratios, which represent yound windsea, occur on the equatorward "frontal" side of the cyclone. A good example of such an inhomogeneous distribution is the low which develops at 65°E, 45°S. In this case a coupling persists beyond the mature stage of the storm. Presumably the storm moves faster than the group velocity of the waves and therefore the wave field never becomes fully developed. In other cases the waves can develop to an equilibrium state, so that at the end of a storm's life cycle the underlying wave field is old. An example is the storm which travels southward at 90°E. High stress ratios are also found westward off the continents, where the fetch is limited in a westerly flow.

We clarify some of the features discussed above in Fig. 2, where time series are shown of the 10-m wind, τ_w/τ and H_s at a north-south section at 51°E for the same time period as in Fig. 1. On the first day a high-pressure system is prevailing at 60°S with a ridge extending equatorward (Fig. 1). At the same time a cyclone is approaching from the west. The passage of the cyclone is reflected by the clockwise rotating wind north of 48°S and by the anti-clockwise rotation south of 48°S. On the equatorward side of the cyclone a "front" appears (37°S, 42°S), with strong surface winds with a maximum wind speed of 24 m/s. Here energetic young windsea with a wave height of 7–8 m and 12-hourly mean $\tau_w/\tau=0.5$ is present. Equatorward of the "front" (31°S) and poleward (48°C, 53°S and 59°S) of the cyclone center the winds are weaker and the wave height and τ_w/τ are lower. The mean wave direction is considerably less variable than the wind direction. In midlatitudes the mean wave direction is determined by swell rather than by windsea. The former tends to propagate in the climatological mean wind direction, whereas the latter follows the daily (high-frequency) wind. Swell propagation out of the storm track is visible in the mean wave direction at lower and higher latitude.

3.2 Time-mean parameters of the sea surface

The July-mean significant wave height as forecast by ECMWF from analyzed winds is shown in Fig 3a. The basic features of this pattern are reproduced by the coupled WAM-ECHAM model (Fig 3b). The mean H_s in the coupled experiment is 3 m in the Southern Ocean storm track except in the southwest Pacific, where the waves and winds are less energetic. The wave height is 1–2 m north of 20°S. Only in the Arabian Sea, where there is storm activity due to the Indian Monsoon, are the waves again 2 m. The coupled model underestimates the mean H_s by about 1 m in the storm areas.

The distribution of the 12-hourly mean τ_w/τ at two latitudes in the Southern Hemisphere (3°S and 42°S) is given in Fig. 4. Windsea with 12-hourly mean $\tau_w/\tau \geq 0.4$ is present 20% of the time at midlatitudes and 5% of the time in the tropics. Windsea with a 12-hourly mean $\tau_w/\tau \leq 0.1$ is present 15% of the time in midlatitudes and 50% of the time in the tropics.

Next we consider the 360-day mean ratio $\overline{\tau_w/\tau}$ (Fig. 5). Over most of the ocean, and in particular over most of the tropical ocean, old windsea prevails. Larger values are found in the Southern Hemisphere storm track, in the Arabian Sea and at some spots in the Northern Hemisphere. Note that the mean wave height (Fig. 3b) is small in part of these areas.

In the Southern Hemisphere storm track the sea surface roughness varies between 0.01 mm and 1 mm in the coupled experiment; the distribution has significantly shifted to larger values and is broader compared to the control experiment (not shown). In the tropics the distribution in the coupled run is not significantly different from the control run (not shown). The 360-day mean sea surface roughness is significantly enhanced (by about 20%) in the coupled run in regions of intense wave generation. The pattern of enhancement (not shown) coincides largely with that of $\overline{\tau_w/\tau}$.

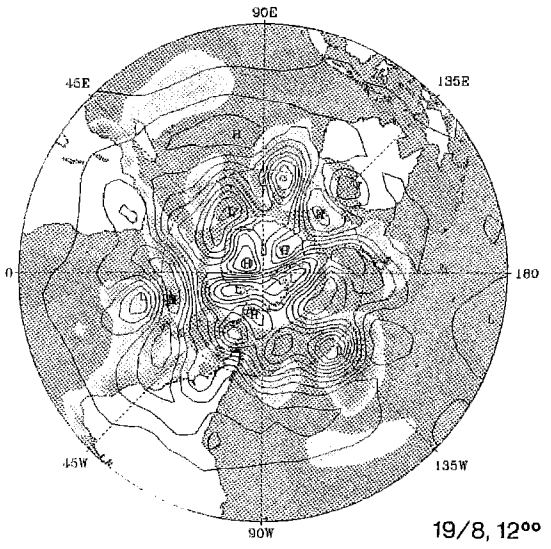

19/8, 12°°

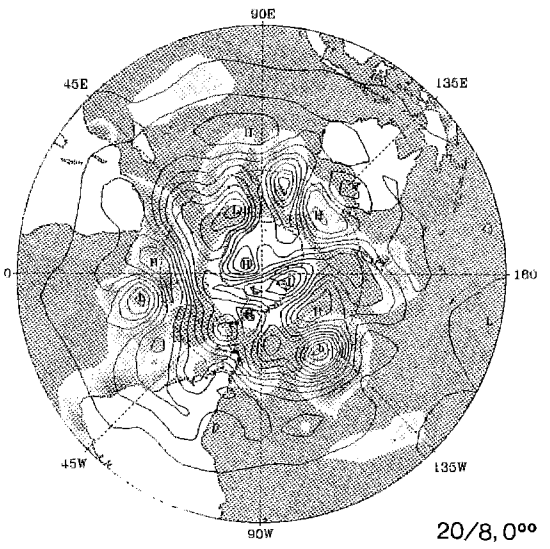

20/8, 0°°

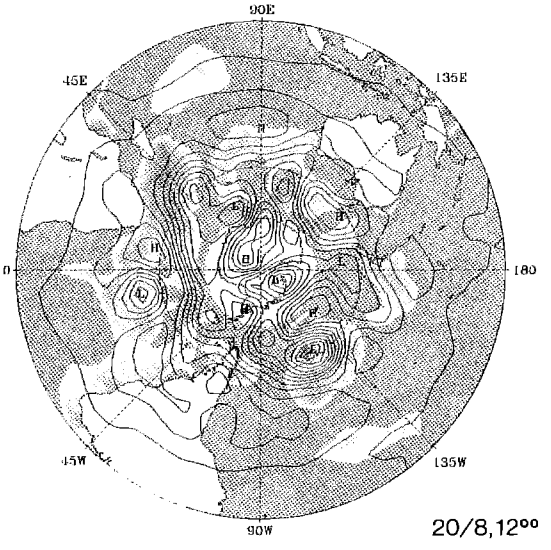

20/8, 12°°

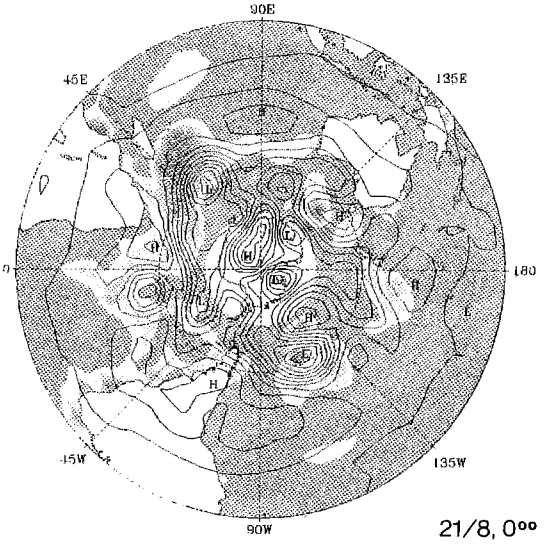

21/8, 0°°

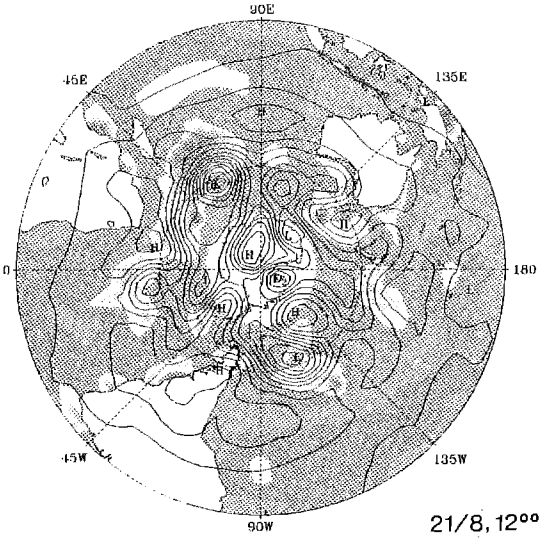

21/8, 12°°

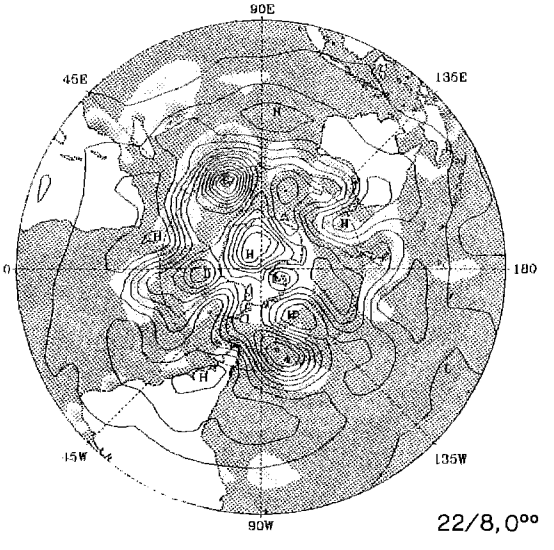

22/8, 0°°

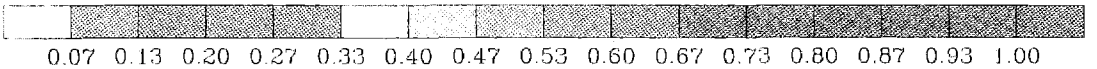

3.3 *Zonally averaged time-mean atmospheric parameters*

Two statistics of the geopotential at 500 hPa are investigated: the 30-day mean and the 2–5 day band-pass filtered variance. There are twelve one-month samples of each in both the control and the coupled experiment. We consider zonally averaged quantities (which are more stable than the latitude-longitude field), because the number of test samples is fairly small. A feedback of the wave model onto the atmospheric flow is most likely to be found in regions where both $\overline{\tau_w/\tau}$ and $\bar{z}_0$ are relatively large. This condition is fulfilled in the Southern Ocean storm belt. However, the signal (the mean of the coupled samples minus the mean of the control samples) is very noisy in both statistics and there are no outstanding features in the belt between 30°S and 60°S.

The statistical stability of the atmospheric response to the space-time variable surface roughness is tested by means of the locally estimated level of recurrence (Storch and Zwiers 1988; see for test procedures Ulbrich et al. 1993). The recurrence test measures the separation between the distribution of the control samples and the distribution of the coupled samples. One assumes that both distributions are Gaussian with means μ_C and μ_W, respectively, and equal variances σ^2. The value of the parameters is estimated from the data. Suppose that $\mu_W > \mu_C$ ($\mu_W < \mu_C$) and that we continue the coupled experiment for one more month. The recurrence test shows the chance that in this month the statistic under consideration will lie above (below) μ_C.

In the present experiment the magnitude of the difference $\mu_W - \mu_C$ is in the storm track about 0.5 σ for both statistics. This implies that the chance for the signal to reoccur in any individual monthly mean of a coupled wave-atmosphere simulation in the storm track is about 70%. The chance that any individual *control* sample lies above (below) the mean value is obviously 50%. It is clear that the two distributions are not well separated in the storm track (or at any other latitude). As an additional test we apply a conventional local t-test. Even with a risk of 10% the null hypothesis $\mu_W = \mu_C$ cannot be rejected with the present small number of independent samples.

From the fact that the signal does not peak in the storm track, where the wave feedback is maximum, and the large overlap between the two distributions we conclude that the differences between the coupled and the control experiment cannot be attributed to the wave model. They reflect random fluctuations in the atmospheric flow.

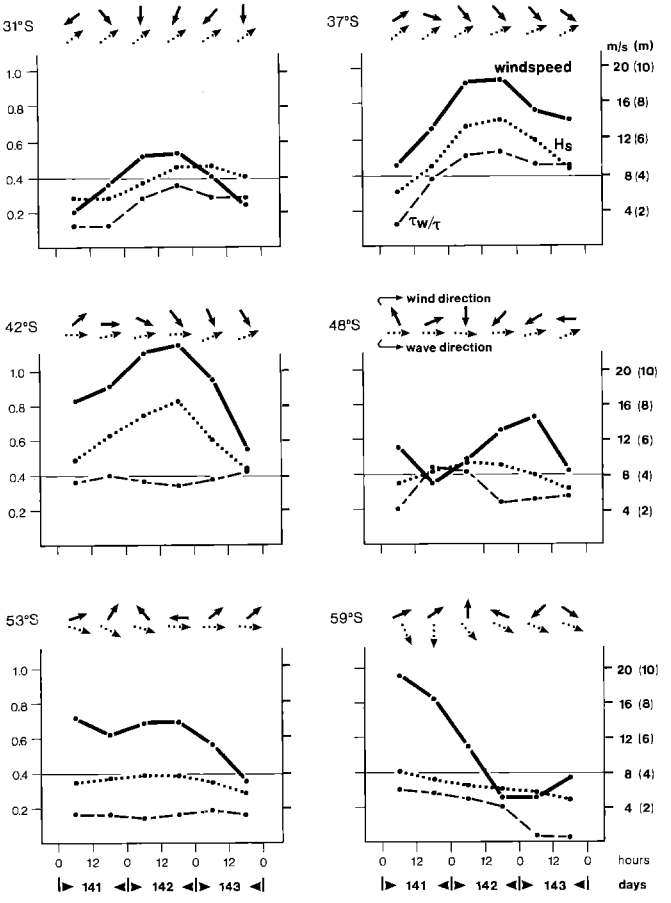

Fig. 2. Time series of the wind speed at 10 m, the stress ratio τ_w/τ and the wave height at six grid points along a north-south section at 51°E for six consecutive time intervals, beginning with day 141 (0–12 UTC) and ending with day 143 (12–24 UTC). Wind and wave direction are indicated, with *arrows* (*solid*, wind; *dotted*, waves) pointing up indicating north. The atmospheric data are 12-hourly means; the wave data are instantaneous. The time-interval coincides with that in Fig. 1

4 Summary and discussion

We have, for the first time, coupled an ocean wave model (WAM) to a climate AGCM (ECHAM) and have integrated it over an extended time. The wave model is forced by the AGCM wind stress whereas the AGCM surface fluxes are modified by the waves, depending on the stress ratio τ_w/τ. The wave field climatology in the coupled experiment is a consistent product of the simulated dynamics of the atmosphere and the waves themselves. The wave heights are realistic. The simulated stress ratio and sea surface roughness seem reasonable. The interaction is weak in the mean in the Southern Hemisphere storm track and negligible everywhere else. The stress ratio exhibits a spatially and temporally highly variable pattern, which is connected to the pattern of lows in the atmospheric flow. This suggests that the evolution of individual storms could be modified by the waves.

The zonally averaged time-mean enhancement of the sea surface roughness is small. During a storm event young windsea is generated in the equatorward

Fig. 1. The sea level pressure and the stress ratio τ_w/τ for 6 consecutive 12-hour periods from the coupled wave-atmosphere model in permanent July mode, beginning with day 141 (0–12 UTC) and ending with day 143 (12–24 UTC). All values are 12-hourly means

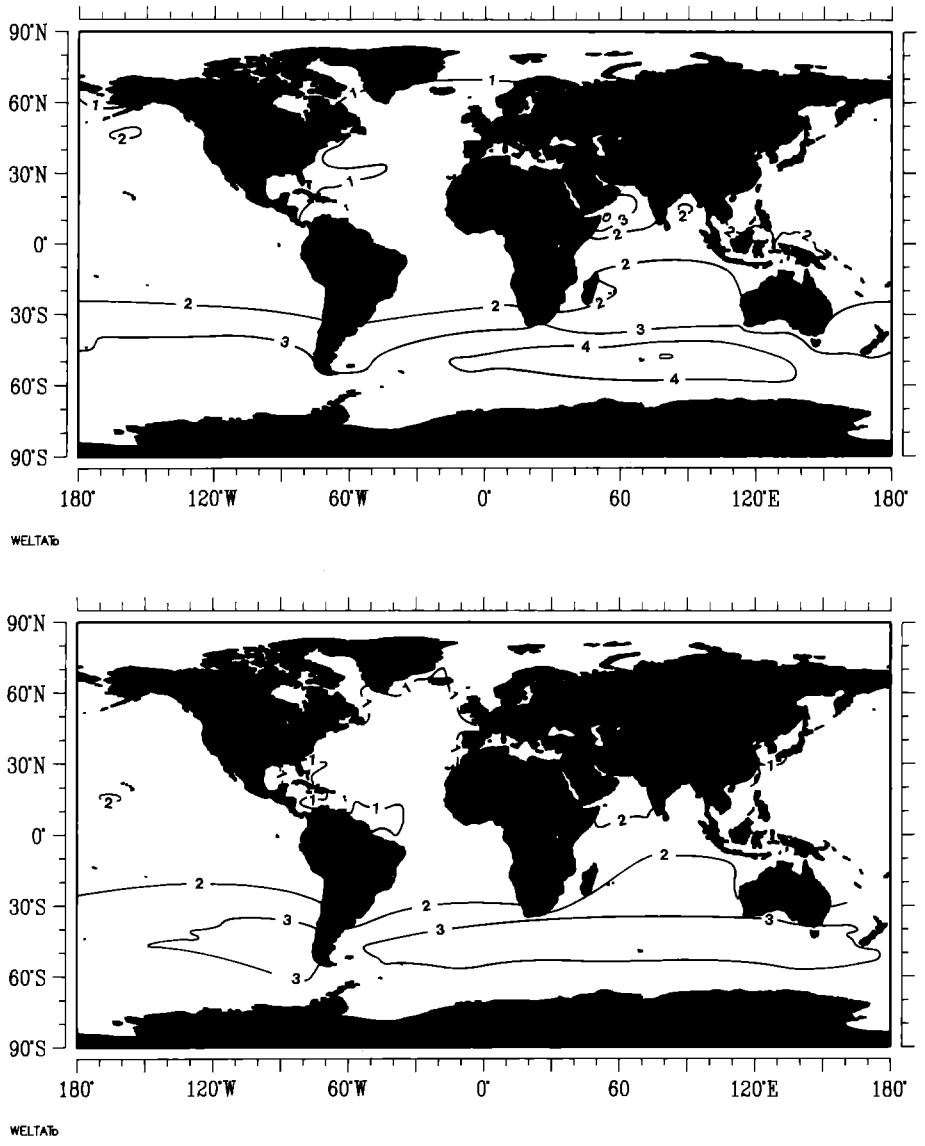

Fig. 3a, b. The July-mean significant wave height $\bar{H}_s$ (in m). **a** as forecast by ECMWF from analyzed winds (mean over July 1987, 1988, 1989 and 1990); **b** as simulated by the coupled wave-atmosphere model (360-day mean)

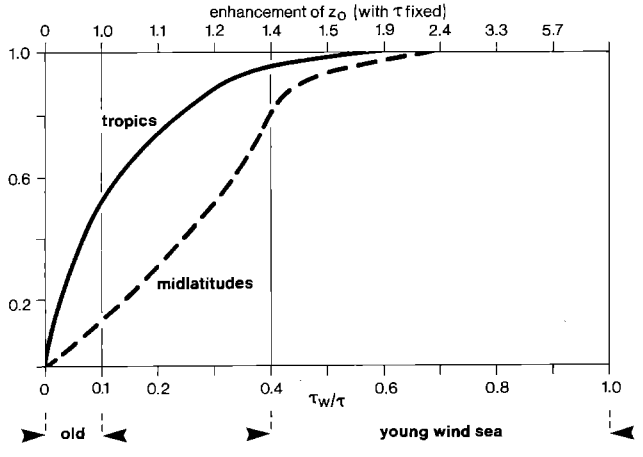

Fig. 4. The distribution function of the 12-hourly mean stress ratio τ_w/τ at a tropical latitude (3° S) and at a storm track latitude (42° S) in the Southern Hemisphere. The interaction between the wave model and the AGCM can be neglected in the tropics (where low stress ratios prevail) and is weak in the mean in midlatitudes (where high stress ratios occur relatively frequent)

area of a cyclone, where a "front" occurs with relatively strong surface winds. The 12-hourly mean roughness enhancement in this area is typically 1.1–1.5, with rare maxima of 3. The atmospheric circulation does not show a statistically stable response to the wave-induced changes in the surface fluxes[1].

It is interesting to compare the present experiment with that made by Ulbrich et al. (1993). They found that a (homogeneous and constant) increase of the sea surface roughness by a factor of ten in the Southern Hemisphere storm track is associated with weakened westerlies and with less, or weaker, storms. Apparently the sea surface roughness *is* a sensitive parameter in a

[1] Note that an earlier version of the present study (Weber et al. 1991) reports a significant response in the atmospheric flow. However, this signal was found to be due to an error in the coupled model. Inadvertently, the ice roughness, which is 1 mm, was replaced by the Charnock relation for open sea. This reduces the surface roughness effectively by an order of magnitude and enhances storm activity, in agremeent with Ulbrich et al. (1993)

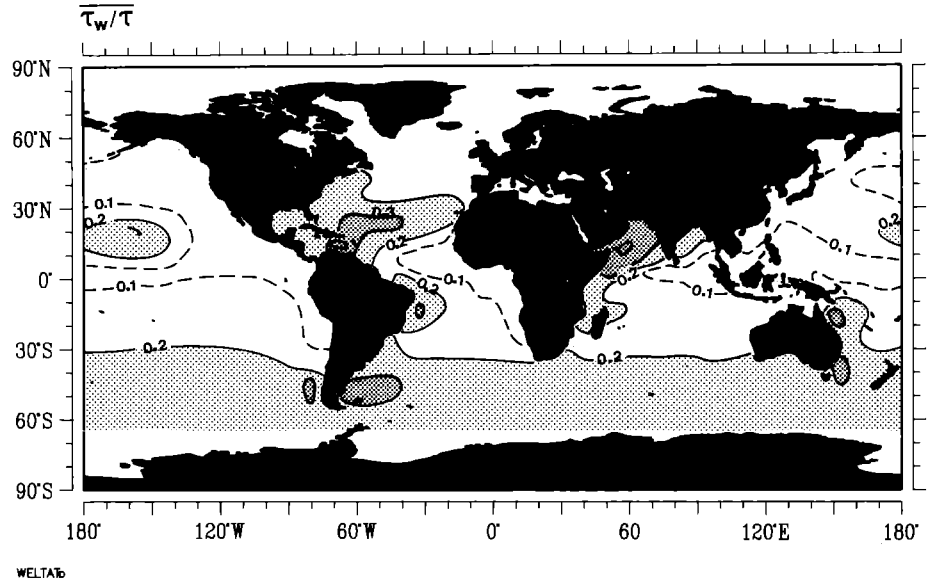

Fig. 5. The 360-day mean ratio $\overline{\tau_w/\tau}$ of the wave-induced stress τ_w to the total stress τ in the coupled wave-atmosphere model. Long-term mean values $\overline{\tau_w/\tau} \leq 0.1$ indicate that the wave field consists almost always of old waves. In areas with $\overline{\tau_w/\tau}=0.2$–$0.3$ young wind sea is relatively frequent present

climate GCM when it is changed by an order of magnitude.

The magnitude and the variabiltiy of the wind are too low in an AGCM with a coarse resolution like T21. Moreover, the time-split integration scheme results in surface stresses which are too weak compared to the surface winds (Janssen et al. 1992). Fortunately, the latter effect seems to be small over sea. The combined effect causes too low wave heights and reduces the possible impact of the coupling, as the wave-induced stress depends on the strength and the variabiliy of the wind. Going to higher resolution and an improved integration scheme it seems unlikely that the time-mean roughness enhancement will be strong enough to change the mean planetary flow directly. However, the interaction between an individual storm and the waves generated by it might become stronger. This might change the baroclinic variance and thus also affect the mean flow.

In state-of-the-art climate AGCMs wave growth is not a relevant process for the large-scale atmospheric circulation.

Acknowledgements. We thank Ulrich Schlese (DKRZ) for his help in setting up the coupled model on the Cray 2 in Hamburg. Peter Janssen helped with advice, and Theo Opsteegh and Reindert Haarsma with their criticism. Heinz Günther (ECMWF) provided the global wave fields as forecast by the ECMWF. Ralph Weisse was bold enough to draw the fronts. Dierk Schriever made the color plots, and Doris Lewandowski and Marion Grunert prepared the diagrams. Grant Branstator critically read an earlier version of the manuscript. The experiments were performed during an eight month stay of SLW at the MPIM in Hamburg; she thanks the MPIM for its hospitality and for providing a very stimulating work environment. Financial support was given through the EC (Grant EPOC 0003-C).

References

Bauer E, Hasselmann SH, Hasselmann K, Graber H (1992) Validation and assimilation of SEASAT altimeter wave heights using the WAM wave model. J Geophys Res 97 (C8):12671–12682

Charnock H (1955) Wind stress on a water surface. Quart J R Meteorol Soc 81:639–640

DeCosmo J (1991) Air-sea exchange of momentum, heat and water vapor over whitecap sea states. PhD-Thesis, University of Washington USA

Hasselmann KH (1991) Ocean circulation and climate change. Tellus 43AB:82–103

Janssen PAEM (1989) Wave-induced stress and the drag of air flow over sea waves. J Phys Oceanogr 19:745–754

Janssen PAEM (1991) Quasi-linear theory of wind generation applied to wave forecasting. J Phys Oceanogr 21:1631–1642

Janssen PAEM, Beljaars ACM, Simmons A, Viterbo P (1992) On the determination of the surface stress in an atmospheric model. Mon Weather Rev 120:2977–2985

Maat N, Kraan C, Oost WA (1991) The roughness of wind waves. Boundary-Layer Meteorol 54:89–103

Miles JW (1957) On the generation of surface waves by shear flows. J Fluid Mech 3:185–204

Roeckner E, Arpe K, Bengtsson L, Brinkop S, Dümenil L, Esch M, Kirk E, Lunkeit F, Ponater M, Rockel B, Sausen R, Schlese U, Schubert S, Windelband M (1992) Simulation of the present-day climate with the ECHAM model: impact of model physics and resolution. Max-Planck-Institut für Meteorologie, Hamburg, Report 93

Romeiser R (1993) Global validation of the wave model WAM over a one-year period using GEOSAT wave height data, J Geophys Res (in press)

Storch H von, Zwiers FW (1988) Recurrence analysis of climate sensitivity experiments. J Clim 1:157–171

Ulbrich U, Bürger G, Schriever D, Storch H von, Weber SL, Schmitz G (1993) The effect of a regional increase in ocean surface roughness on the tropospheric circulation: a GCM experiment. Clim Dyn 8:277–285

Wamdig (1989) The WAM model – a third generation ocean wave prediction model. J Phys Oceanogr 18:1775–1810

Weber SL, Storch H von, Viterbo P, Zambresky L (1991) Coupling an ocean wave model to an atmospheric general circulation model. Max-Planck-Institut für Meteorologie, Hamburg, Report 72

Zambresky L (1989) A verification study of the global WAM model December 1987–November 1988. ECMWF Technical Report 6